AN UNCONDITIONALLY STABLE, ENERGY PRESERVING METHOD FOR MAGNETOHYDRODYNAMICS

J.A. Hopman[1], J. Rigola[1] and F.X. Trias[1]

[1] **_Heat and Mass Transfer Technological Center, Technical University of Catalonia ESEIAAT, c/Colom 11, Terrassa, 08222, Barcelona, Spain_**

jannes.hopman@upc.edu

March 17, 2025

1 Introduction

Accurate simulation tools for magnetohydrodynamic (MHD) flows at low magnetic Reynolds number are of great interest for many industrial applications, such as in the design of nuclear fusion reactors [Hoshino *et al.* (2011)]. Extreme circumstances created inside the reactor limit the use of experimental techniques, leaving numerical modeling as the method of choice [Abdou *et al.* (2001)]. The interaction of the conductive fluids with magnetic fields, leads to an opposing Lorentz force. Accurate numerical schemes which conserve physical properties such as mass, momentum, kinetic energy and charge density, are of great importance when modeling the delicate balance between the high pressure drop and the opposing Lorentz force. The opposing Lorentz force is stronger at the center of the flow, which can create quasi-two-dimensional turbulence effects at high Reynolds numbers [Smolentsev *et al.* (2015)]. In these cases, conservative schemes are essential in depicting turbulent transition in space and time, since numerical dissipation greatly affects the small scale flow structures which form the basis of turbulence [Verstappen and Veldman (2003)]. The often complex geometries found in industrial applications require a collocated grid approach, which, combined with low-dissipative schemes for incompressible flows, can lead to the checkerboard problem [Trias *et al.* (2014)]. The problem finds its origins in the discrete collocated gradient and Laplacian operators, which are insensitive to high-frequency modes in the pressure [Hopman *et al.* (2025)]. This problem becomes more relevant in MHD at low magnetic Reynolds numbers, since an additional Poisson equation is formed to solve the electric potential field. In most finite volume codes, the classical Rhie-Chow interpolation and a compact-stencil Laplacian operator are used to minimise the checkerboard problem at the cost of adding numerical dissipation. A low-dissipative method for MHD is developed, which quantifies the checkerboard problem and allows numerical dissipation in the solution accordingly, and thereby maintains high accuracy and unconditional stability. This numerical framework is presented in section 2. The method is tested on a turbulent duct flow benchmark case with a conductive fluid and a transverse magnetic field. Some preliminary test results are presented in section 3.

2 Numerical Framework

A fractional step method forms the basis of the numerical scheme, of which the equations are given in algorithm 1. The discretisation of the algebraic operators can be found in [Hopman *et al.* (2025)], with the physical variables given by: collocated velocity, $\mathbf{u}_c$, staggered velocity, $\mathbf{u}_s$, modified kinematic pressure $\tilde{\mathbf{p}}_c$, current density, $\mathbf{J}_c$, magnetic field, $\mathbf{B}_c$, electric potential, $\boldsymbol{\phi}_c$, density, ρ, and electrical conductivity, σ. The discrete operators are given by: collocated gradient, G_c. face gradient, G, collocated divergence, M_c, compact-stencil Laplacian, L, cell-to-face dot-interpolator, Γ_{cs} and face-to-cell interpolator, Γ_{sc}. Treatment of the temporal discretisation is left out of scope, and the temporal treatment of the convective and diffusive terms are included in function $\mathcal{F}(\mathbf{u}_c, \mathbf{u}_s)$. $[\cdot]_\times$ gives a skew-symmetric matrix form of a vector field which enables the cell-wise cross product between two vector fields.

$$\mathbf{u}_c^p = \mathcal{F}(\mathbf{u}_c, \mathbf{u}_s) - G_c\tilde{\mathbf{p}}_c^p + \frac{1}{\rho}[\mathbf{J}_c^n \times \mathbf{B}_c^n] \tag{A1.1}$$

$$L\tilde{\mathbf{p}}_c' = M_c\mathbf{u}_c^p \tag{A1.2}$$

$$\mathbf{u}_s^{n+1} = \Gamma_{cs}\mathbf{u}_c^p - G\tilde{\mathbf{p}}_c' \tag{A1.3}$$

$$\mathbf{u}_c^{n+1} = \mathbf{u}_c^p - G_c\tilde{\mathbf{p}}_c' \tag{A1.4}$$

$$\tilde{\mathbf{p}}_c^{n+1} = \tilde{\mathbf{p}}_c^p + \tilde{\mathbf{p}}_c' \tag{A1.5}$$

$$\mathbf{J}_c^p = \sigma([\mathbf{u}_c^{n+1}] \times \mathbf{B}_c^n - G_c\boldsymbol{\phi}_c^p) \tag{A1.6}$$

$$L\boldsymbol{\phi}_c' = M_c\mathbf{J}_c^p/\sigma \tag{A1.7}$$

$$\mathbf{J}_c^{n+1} = \Gamma_{sc}(\Gamma_{cs}\mathbf{J}_c^p - \sigma G\boldsymbol{\phi}_c') \tag{A1.8}$$

$$\boldsymbol{\phi}_c^{n+1} = \boldsymbol{\phi}_c^p + \boldsymbol{\phi}_c' \tag{A1.9}$$

Algorithm 1: Symmetry-preserving algorithm for MHD flows

Compared to well-known hydrodynamic versions of algorithm 1, the MHD part only consists of an extra source term in the form of a Lorentz force in equation (A1.1), and equations (A1.6)-(A1.9), in which a second Poisson equation for the electromagnetic quantities is posed and solved. The definition of the face-to-cell interpolator, Γ_{sc}, in equation (A1.8) plays a crucial role in the conservation of charge density, and prevents numerical dissipation through the form of Lorentz work. In this framework, the definition is linked to the cell-to-face dot interpolator, Γ_{cs}, by:

$$\Gamma_{sc} = \Omega^{-1}\Gamma_{cs}^{T}\Omega_{s}, \tag{1}$$

with volumetric interpolation between cell-centers and faces, Γ_{cs}, to ensure unconditional stability [Santos *et al.* (2025)]. This is in contrast with the definition by [Ni *et al.* (2007)]:

$$\left[\Gamma_{sc}^{Ni}\mathbf{v}_{s}\right]_{i} = \sum_{f\in F_{f}(i)} \frac{A_{f}\left(\mathbf{r}_{f}-\mathbf{r}_{i}\right)}{\Omega_{c}}\left[\mathbf{v}_{s}\right]_{f}, \tag{2}$$

where $\mathbf{r}_f - \mathbf{r}_i$ gives the vector from cell-center i to face-center f, for which the relation given in equation (1) does not hold.

Addition of the predictor fields for p and ϕ in equations (A1.1) and (A1.6) can increase the order of the numerical errors and lower the numerical dissipation. However, setting these predictor values to the values at the previous time-step can cause checkerboarding in the solution fields. Therefore, by quantifying the checkerboard problem, a coefficient can be calculated which directly couples back to the predictor value. Thereby establishing a negative feedback mechanism which is able to dynamically balance the checkerboard problem with numerical dissipation. The predictor values in the final algorithm are defined by:

$$\boldsymbol{\alpha}_{c}^{p} = \left(1-\alpha_{cb}\right)\boldsymbol{\alpha}_{c}^{n}, \tag{3}$$

where α represents the pressure or electric potential field. α_{cb} gives the quantity of checkerboarding of the respective fields, and is calculated as:

$$\alpha_{cb} = \frac{\boldsymbol{\alpha}_{c}^{T}\left(L-L_{c}\right)\boldsymbol{\alpha}_{c}}{\boldsymbol{\alpha}_{c}^{T}L\boldsymbol{\alpha}_{c}}, \tag{4}$$

with $\alpha_{cb} = 0$ if the denominator equals zero. This symmetry-preserving algorithm with dynamical treatment of the checkerboarding was compared to a method which uses equation (2) to interpolate the charge density, and which does not have the dynamical treatment of the predictor fields.

The solver is implemented in open source software OpenFOAM, and made available under *RKSymMagFoam* at [Hopman and Frederix (2003)].

3 Results

Preliminary tests were performed using a turbulent duct flow case, with insulated walls [Shercliff (1953)] at $Re_B = 5602$ and $Ha = 21.2$. The fluid flows along the duct in the x-direction, whereas the magnetic field is applied in the y-direction. The simulation was first performed on a high resolution Cartesian mesh, similar to [Zhang *et al.* 2015], to establish reference results. The simulations were then performed again on a non-Cartesian mesh with eight times less control volumes. This was done to see a difference in the interpolation method, as they converge to the same method on Cartesian meshes. Moreover, unstructured grids are more common in industrial cases with complex geometries. These meshes are also more prone to the checkerboard problem, which gives a good method to see the difference between the solvers. The newly introduced solving algorithm is denoted by SP-θ_{dy}, to indicate the symmetry-preserving (SP) discretisation with the dynamic (dy) predictor values. This solver is compared to a non-symmetry-preserving (NSP) equivalent, without the dynamic predictor values.

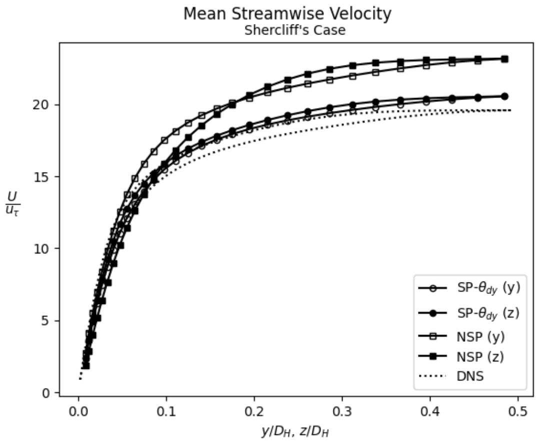

Figure 1: Mean streamwise velocity profiles in y and z, for the two solvers

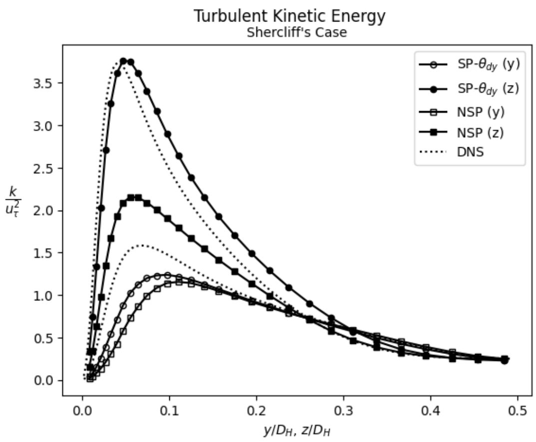

Figure 2: Turbulent kinetic energy profiles in y and z, for the two solvers

Figure 1 shows the mean velocity profiles. The DNS shows a clear distinction between the y- and z-

profiles, which is due to the magnetic field applied in the y-direction. The influence of the coarse non-Cartesian mesh can be seen in an elevated velocity profile, especially at the center of the duct. This indicates lower levels of turbulence due to numerical dissipation, as the profiles are closer to the laminar parabolic shape. This effect is mostly visible for the NSP solver, which indicates that the symmetry preserving interpolator has a beneficial effect on the conservational properties of the solver. The turbulent kinetic energy profiles, seen in figure 2, confirm these findings, showing a large deficit for the NSP solver, especially close to the wall in the z-profile.

	SP-θ_{dy}	NSP
p_{cb}	0.5	0.9
ϕ_{cb}	0.6	0.6

Table 1: Checkerboard coefficient for the pressure and electric potential fields

From the quantification of the checkerboard values of the pressure and electric potential fields, given in table 1, a distinction can also be seen for the amount of pressure checkerboarding. The checkerboarding is suppressed dynamically in the SP-θ_{dy} solver, resulting in a lower value. This might also contribute to a higher numerical dissipation in the NSP solver, which leads to the results seen in figures 1 and 2.

To expand on this analysis, other test cases will be run, using other combinations of the checkerboard treatment and (non-)symmetry-preserving interpolator. These results will be presented using analysis of the higher order statistical terms, including the turbulent kinetic energy budgets, to give a better understanding of the causes and effects of the chosen numerical method.

Acknowledgements This work is supported by the SIMEX project (PID2022-142174OB-I00) of *Ministerio de Ciencia e Innovación* and the RETOtwin project (PDC2021-120970-I00) of *Ministerio de Economía y Competitividad*, Spain. J.A.H. is supported by the FI AGAUR-Generalitat de Catalunya fellowship (2023 FI_B1 00204), financed and extended by *Universitat Politècnica de Catalunya* and *Banc Santander*. The numerical experiments have been conducted on the Marenostrum5 supercomputer at the *Barcelona Supercomputing Center* under the project IM-2024-3-0019. The authors thankfully acknowledge these institutions.

References

Abdou, M. A., Ying, A., Morley, N., Gulec, K., Smolentsev, S., Kotschenreuther, M., Malang, S., Zinkle, S., Rognlien, T., Fogarty, P., Nelson, B., Nygren, R., McCarthy, K., Youssef, M. Z., Ghoniem, N., Sze, D., Wong, C., Sawan, M., Khater, H., Woolley, R., Mattas, R., Moir, R., Sharafat, S., Brooks, J., Hassanein, A., Petti, D., Tillack, M., Ulrickson, M., and Uchimoto, T. (2001), On the exploration of innovative concepts for fusion chamber technology, *Fusion Eng. Des.*, Vol. 54, No. 2, pp. 181–247.

Hopman, J. A., Santos, D., Alsalti-Baldellou, A., Rigola, J., and Trias, F. X. (2025), Quantifying the checkerboard problem to reduce numerical dissipation, *J. Comput. Phys.*, Vol. 521, p. 113537.

Hopman, J. A., Frederix, E. M. A., RKSymFoam GitHub page (2023), URL `https://github.com/janneshopman/RKSymFoam`

Hoshino, T., Kato, K., Natori, Y., Oikawa, F., Nakano, N., Nakamura, M., Sasaki, K., Suzuki, A., Terai, T., and Tatenuma, K. (2011), Development of advanced tritium breeding material with added lithium for ITER-TBM, *J. Nucl. Mater.*, Vol. 417, No. 1-3, pp. 684–687.

Ni, M. J., Munipalli, R., Morley, N. B., Huang, P., and Abdou, M. A. (2007), A current density conservative scheme for incompressible MHD flows at a low magnetic Reynolds number. Part I: On a rectangular collocated grid system, *J. Comput. Phys.*, Vol. 227, No. 1, pp. 174–204.

Santos, D., Hopman, J. A., Pérez-Segarra, C. D., and Trias, F. X. (2025), On a symmetry-preserving unconditionally stable projection method on collocated unstructured grids for incompressible flows, *J. Comput. Phys.*, Vol. 523, p. 113631.

Sherclif, J. A. (1953), Steady motion of conducting fluids in pipes under transverse magnetic fields, *Math. Proc. Camb. Philos. Soc.* Vol. 49, No. 1, pp. 136-144.

Smolentsev, S., Badia, S., Bhattacharyay, R., Bühler, L., Chen, L., Huang, Q., Jin, H. G., Krasnov, D., Lee, D. W., Les Valls, E. M. De, Mistrangelo, C., Munipalli, R., Ni, M. J., Pashkevich, D., Patel, A., Pulugundla, G., Satyamurthy, P., Snegirev, A., Sviridov, V., Swain, P., Zhou, T., and Zikanov, O. (2015), An approach to verification and validation of MHD codes for fusion applications, *Fusion Eng. Des.*, Vol. 100, pp. 65–72.

Trias, F. X., Lehmkuhl, O., Oliva, A., Pérez-Segarra, C. D., and Verstappen, R. W. (2014), Symmetry-preserving discretization of Navier–Stokes equations on collocated unstructured grids, *J. Comput. Phys.*, Vol. 258, pp. 246–267.

Verstappen, R. W., and Veldman, A. E. (2003), Symmetry-preserving discretization of turbulent flow, *J. Comput. Phys.*, Vol. 187, No. 1, pp. 343–368.

Zhang, H. Trias, F. X., Gorobets, A., Tan, Y., Oliva, A. (2015), Direct numerical simulation of a fully developed turbulent square duct flow up to $Re_\tau = 1200$, *Int. J. Heat Fluid Flow*, Vol. 54, pp. 258-267.